

VLASOV ANALYSIS OF MICROBUNCHING GAIN FOR MAGNETIZED BEAMS*

C.-Y. Tsai[#], Department of Physics, Virginia Tech, VA 24061, USA

Ya. Derbenev, D. Douglas, R. Li, and C. Tennant Jefferson Lab, Newport News, VA 23606, USA

Abstract

For a high-brightness electron beam with low energy and high bunch charge traversing a recirculation beamline, coherent synchrotron radiation and space charge effect may result in the microbunching instability (MBI). Both tracking simulation and Vlasov analysis for an early design of Circulator Cooler Ring [1] for the Jefferson Lab Electron Ion Collider reveal significant MBI. It is envisioned these could be substantially suppressed by using a magnetized beam. In this work, we extend the existing Vlasov analysis, originally developed for a non-magnetized beam, to the description of transport of a magnetized beam including relevant collective effects. The new formulation will be further employed to confirm prediction of microbunching suppression for a magnetized beam transport in a recirculating machine design.

INTRODUCTION

Beam quality preservation is of general concern in delivering a high-brightness electron beam through a transport line or recirculation arc in the design of modern accelerators. During high-brightness beam transport, initial small density modulations can be converted into energy modulations due to short-ranged wakefields or high-frequency impedances. Then, the energy modulations can be transformed back to density counterparts downstream in dispersive regions. The density-energy conversion, if forming a positive feedback, can result in the enhancement of modulation amplitudes. This has been known as the microbunching instability (MBI) (see, for example, Refs. [2-4]). MBI has been one of the most challenging issues associated with beamline designs such as magnetic bunch compressor chicanes for free-electron lasers or linear colliders. Moreover, it also poses difficulties in the design of transport lines for recirculating or energy-recovery-linacs (ERLs). Any dominant source of beam performance limitations in such a high-brightness electron beam transport system must be carefully examined in order to preserve beam phase-space quality. Among those, we already know the longitudinal space charge force (LSC) and coherent synchrotron radiation (CSR) can, in particular, drive MBI. The LSC effect stems from upstream ripples on top of the longitudinal charge density, and can generate an energy modulation when the beam traverses a long section of a beamline. When the beam encounters bending, CSR due to electron coherent radiation emission inside a bend can

have a significant effect upon further amplifying the induced density modulations. A typical transport line in a recirculated machine can have a long linac or straight section and a large number of bending dipoles, and thus can potentially incubate such density-energy conversion along the beamline. The successive accumulation and conversion mechanism between density and energy modulations can result in significant microbunching amplification.

In the early design of the Circulator Cooler Ring (CCR) [1] for the Jefferson Lab Electron Ion Collider (JLEIC) [5], both tracking simulations [6, 7] and Vlasov analysis [8, 9] have shown that MBI is a serious concern for the CCR design. The one-turn CSR microbunching gain (to be defined later) is found to be up to 4000 at the modulation wavelength of 350 μm and is even higher when LSC is included. This is mainly due to the high bunch charge (~ 2 nC) and relatively low energy (~ 55 MeV) of the cooling beam circulating in the CCR. Mitigation of MBI thus becomes an issue for a high-brightness beam transport in recirculating machines. Several mitigation schemes have been proposed in the literature for different machine configurations and can be in general divided into two categories: those addressing the transport lattice, and those directed at the transported beam. For the former aspect, the optics impact of beamline lattice designs on MBI has been recently investigated [10-15]. In those beamline designs, the beam is transversely uncoupled, i.e. non-magnetized. For the latter aspect, Derbenev [16] had proposed using magnetized beam to improve electron cooling performance [17] and to mitigate collective effects such as space charge [18] and MBI (our primary focus in this paper). A magnetized beam can be generated by immersing the cathode in an axial magnetic field and thus features a nonzero angular momentum. In general, the magnetized beam is a transversely coupled beam.

In the remainder of this paper, we will derive the equations governing microbunching for a transversely coupled beam. Our derivation largely follows the theoretical treatment by Huang and Kim [4] and Heifets, Stupakov, and Krinsky [3]. To characterize the general feature of a magnetized (or a otherwise coupled) beam, we use the beam sigma matrix instead of Twiss (or Courant-Snyder) parameters. We then apply the resultant integral equation to a specialized arc design for magnetized beam transport to a section of cooling solenoid. We also benchmark our developed code against particle tracking by ELEGANT [19]. Both simulation results are in good agreement.

* This material is based upon work supported by the U.S. Department of Energy, Office of Science, Office of Nuclear Physics under contract DE-AC05-06OR23177.

[#]jcytsai@vt.edu

THEORETICAL FORMULATION

A convenient way to characterize a transversely coupled beam is to consider its moments [20]. In many cases, the 6-D beam phase space distribution function is quadratic in the phase space coordinates. For our discussion, we define \mathbf{X} and \mathbf{X}_{4D} as $\mathbf{X}(s) = (x, x', y, y', z, \delta; s)$ and $\mathbf{X}_{4D}(s) = (x, x', y, y'; s)$, respectively. The system Hamiltonian is assumed to have a quadratic form to \mathbf{X} . Given the Hamiltonian the solution to the system, in the absence of collective effect, to first order, can be expressed as

$$\mathbf{X}(s) = R(s)\mathbf{X}(0) \quad (1)$$

where R is the linear transport matrix.

For a collection of particles, we use the phase-space distribution function f to describe the beam behavior. If the collision between particles is ignored, the evolution is governed by Vlasov equation. The unperturbed solution

$$f(\mathbf{X}(s); s) = f(\mathbf{X}(0); 0) = f(R^{-1}(s)\mathbf{X}(s); 0). \quad (2)$$

The electron phase-space distribution is assumed to be Gaussian in (x, x', y, y', δ) and uniform in z

$$\bar{f}_0(\mathbf{X}_0) = \frac{n_0}{(2\pi)^{5/2} \varepsilon_{4D}^2 \sigma_\delta} \exp \left\{ -\frac{1}{2} \mathbf{X}_{4D,0}^T \Sigma_{4D}^{-1} \mathbf{X}_{4D,0} - \frac{(\delta_0 - h z_0)^2}{2\sigma_\delta^2} \right\} \quad (3)$$

where Σ_{4D} is the beam sigma matrix and $\varepsilon_{4D} = \sqrt{\det(\Sigma_{4D})}$ is the 4-D beam emittance. σ_δ is the uncorrelated relative rms energy spread and h is the chirp on the beam.

Assume the beam phase space is perturbed during infinitesimal time duration $d\tau$ due to an energy kick $d\delta$ from collective effects. Ignoring $\partial f_0 / \partial \delta$ and summing up this contribution over the entire trajectory gives [4]

$$f(\mathbf{X}; s) = f_0(\mathbf{X}_0) - \int_0^s d\tau \frac{\partial f_0(\mathbf{X}_\tau)}{\partial \delta_\tau} \frac{d\delta}{d\tau}. \quad (4)$$

We are interested in the microbunching development along a beamline; microbunching can be quantified by the Fourier transform of perturbed phase-space distribution function (or, bunching factor)

$$b(k_z; s) = \frac{1}{N} \int d\mathbf{X} e^{-ik_z z_s} f(\mathbf{X}; s). \quad (5)$$

Our goal is to derive the governing equation for $b(k_z; s)$ by substituting Eqs.(3) and (5) into (4). This involves an integral of the form (assume initial density modulation, $f_0^{(z)} = (1 + \Delta n/n_0) \bar{f}_0$)

$$\int d\mathbf{X}_{4D,0} dz_0 d\delta_0 f_0^{(z)}(\mathbf{X}_{4D,0}, z_0, \delta_0) e^{-ik_z z_s}. \quad (6)$$

Direct integration of the Eq. (6) becomes awkward. To simplify, we can diagonalize the exponent in Eq. (6). First, we define a set of de-coupled 4-D phase-space coordinates as $\mathbf{U}_0 = (u_1, u_2, u_3, u_4)$ so that the transformation from \mathbf{X}_0 to \mathbf{U}_0 satisfies the following criterion $\mathbf{V} \Sigma_{4D}^{-1} \mathbf{V}^{-1} = D^{-1}$ where D is a diagonal matrix

with $\det(D^{-1}) = \det(\Sigma_{4D}^{-1})$, $\det(\mathbf{V}) = 1$, $\mathbf{V}^T = \mathbf{V}^{-1}$. After the coordinate transformation, the term in the exponent of Eq. (3) becomes

$$\mathbf{X}_{4D,0}^T \Sigma_{4D}^{-1} \mathbf{X}_{4D,0} = \mathbf{U}_0^T D^{-1} \mathbf{U}_0 \quad (7)$$

and the term z_s in Eq. (6),

$$z_s = \sum_{j=1}^4 R_{5j}(s) X_0^j + R_{55}(s) z_0 + R_{56}(s) \delta_0 = \sum_{j=1}^4 \sum_{i=1}^4 R_{5j}(s) V_{ji}^{-1} u_i + R_{55}(s) z_0 + R_{56}(s) \delta_0 \quad (8)$$

Now the exponent becomes de-coupled and the integration over \mathbf{U}_0 can be easily done. By substituting Eq. (4) into Eq. (5), we arrive at the governing equation for microbunching in terms of $b(k_z; s)$,

$$b(k_z; s) = b_0(k_z; s) + \int_0^s d\tau K^{MAG}(\tau, s) b(k_z; \tau) \quad (9)$$

where $b_0(k_z; s) = b_0(k_z; 0) \{L.D.; s, 0\}$ and

$$K^{MAG}(\tau, s) = \frac{ik_z(s)I(\tau)}{\gamma I_A} R_{56}(\tau \rightarrow s) Z(k_z; \tau) \{L.D.; s, \tau\} \quad (10)$$

where $I(\tau)$ is the peak current at $s = \tau$, I_A the Alfven current, γ the relativistic factor, $Z(k)$ is the impedance per unit length. Landau damping is expressed as

$$\{L.D.; s, \tau\} = \exp \left\{ -\frac{k_0^2}{2} \sum_{i=1}^4 \frac{1}{D_{ii}^{-1}} \left(\sum_{j=1}^4 \Re_{5j}(s, \tau) V_{ji}^{-1} \right)^2 - \frac{k_0^2}{2} \Re_{56}^2(s, \tau) \sigma_\delta^2 \right\} \quad (11)$$

$$\Re_{5j}(s, \tau) = C(s) R_{5j}(s) - C(\tau) R_{5j}(\tau), j = 1, 2, 3, 4, 6 \quad (12)$$

$C(s)$ is the compression factor and $R_{56}(\tau \rightarrow s)$ can be obtained by $\mathbf{R}(\tau \rightarrow s) = \mathbf{R}(s) \mathbf{R}^{-1}(\tau)$.

Equation (9) is a compact integral equation that governs the microbunching process. The quantity of particular interest is the microbunching gain, defined as the ratio of bunching factors at a certain location s to the initial location $s = 0$,

$$G(s) \equiv \left| \frac{b(k_z; s)}{b_0(k_z; 0)} \right|. \quad (13)$$

Hereafter, we call $G(s)$, the *gain function*, which is a function of s for a given modulation wavenumber, and refer to $G_f(\lambda) = G(s = s_f; \lambda = 2\pi/k_z)$ as the *gain spectrum*, a function of modulation wavelength at the exit location of a lattice (the subscript “ f ” indicates the exit of a beamline).

To summarize the general physical mechanism of MBI as described by Eqs. (9-11): a density perturbation at τ induces an energy modulation through the $Z(k, \tau)$, and is subsequently converted into density modulation at s through the momentum compaction function $R_{56}(\tau \rightarrow s)$ [4].

EXAMPLE

In this section we illustrate the microbunching gain analyses by considering an example arc lattice for magnetized beam transport. Table 1 summarizes initial beam parameters used in our simulations. This achromatic arc is composed of eight cells, and each cell is constructed by two inward and one outward bends. The total bending angle is 180 degrees. Each bending dipole is designed as a

half-indexed [21] and combined-function dipole. The arc lattice serves to transport the beam, to match toward the downstream solenoid entrance [22], as well as to preserve the axial symmetry.

Table 1: Initial Beam Parameters used in the Simulation

Name	Value	Unit
Beam energy	55	MeV
Initial peak bunch current	22.5	A
4-D geometric emittance	1.11×10^{-7}	M
Compression factor	0.28	
Chirp	4.465	
Energy spread (uncorrelated)	1.5×10^{-4}	

Figure 1 shows the simulation results for the arc example. A nonzero chirp is imposed to the beam so that the bunch is de-compressed when it traverses through the arc. The evolution of bunch current is shown in Fig. 1(a). The microbunching gain function, defined in Eq. (13), is illustrated in Fig. 1(b), for $\lambda = 300 \mu\text{m}$. In this figure, the dots are obtained from ELEGANT tracking, in which 16-million simulation particles are used and 700 bins are set to ensure the convergence of the results and the minimum resolved modulation wavelength down to $50 \mu\text{m}$. The input beam phase-space distribution for particle tracking is prepared according to Ref. [23]. The data postprocessing follows that described in Ref. [24] and for detailed procedures we refer to Ref. [25]. In the simulation, we only incorporate the free-space 1-D steady-state CSR effect [26, 27]. Figure 1(c) shows the microbunching gain spectrum, as a function of modulation wavelength at the exit of the arc. From Figs. 1(b) and 1(c) we can see both our Vlasov solutions and tracking results agree with each other. The analysis shows that there is basically no gain growth along the arc. As a reference, Fig. 1(d) indicates the validity of 1-D CSR model [26] used in the simulation. The Derbenev ratio is defined as $\kappa = \sigma_x / \lambda^{2/3} \rho^{1/3}$. The ratio is assumed to be small when 1-D model is valid. When the ratio is no longer small, the transverse variation of the CSR field needs to be taken into account, and a 2-D CSR model is required [28, 29].

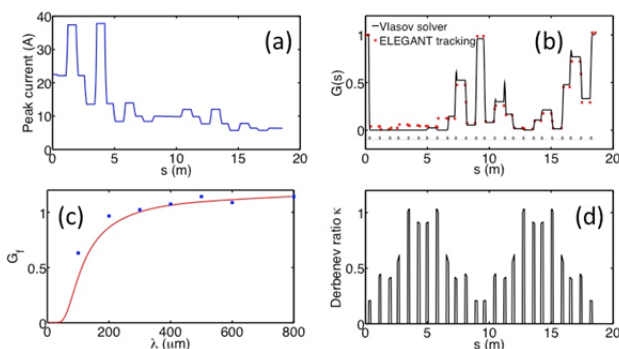


Figure 1: (a) bunch decomposition along the arc; (b) gain function for $\lambda = 300 \mu\text{m}$; (c) gain spectrum; (d) Derbenev ratio as a function of s . Note, in the simulation results, only steady-state CSR is included.

5: Beam Dynamics and EM Fields

D05 - Coherent and Incoherent Instabilities - Theory, Simulations, Code Developments

Compared to a non-magnetized beam, a general feature of a magnetized beam is the (much) larger transverse beam size because of its intrinsic angular momentum. This larger beam size can have a smearing effect at locations where $R_{51}\sigma_x > \lambda$. In this arc example, $R_{51}\sigma_x \approx 2 \text{ mm}$, much longer than the modulation wavelength of interest [30]. A conceptual illustration is shown in Fig. 2. The smearing effect is similar to that due to large slice energy spread with $R_{56}\sigma_\delta > \lambda$. It is this larger transverse beam size that helps mitigate the MBI in our situation.

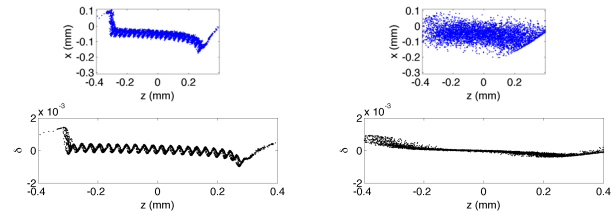


Figure 2: Illustration of R_{51} -smearing effect due to small (left) and large (right) transverse beam size as the beam traverses a dipole. In the figure, the transverse emittance is set the same for the two cases but the beam sizes are different. In the left figure, $R_{51}\sigma_x \approx 10 \mu\text{m}$, while $R_{51}\sigma_x \approx 100 \mu\text{m}$ in the right figure. The modulation wavelength is assumed $30 \mu\text{m}$.

SUMMARY

We have derived a semi-analytical equation for microbunching analysis of general transversely coupled beams. The theoretical treatment we followed is largely from Refs. [3,4]. Solution to the integral equation has been benchmarked against particle tracking simulation; they show excellent agreement. An arc lattice, designed to transport a magnetized beam for downstream cooling, is shown to have nearly no microbunching gain. A more complete analysis will be carried out when a full-ring lattice is provided.

We have shown that our Vlasov solver can be used for quick estimates of microbunching in magnetized beam transport, and for subsequent optimization of beamline design when MBI is a concern. This can be done without tracking a large number of simulation particles.

ACKNOWLEDGMENTS

We thank Steve Benson for his coordination of this work and stimulating discussion. This work is supported under U.S. DOE Contract No. DE-AC05-06OR23177.

REFERENCES

- [1] Ya. Derbenev and Y. Zhang, "Electron cooling for electron ion collider at JLab", in *Proc. of COOL'09*, Lanzhou, China, 2009, paper FRM2MCCO01.
- [2] M. Borland, "Start-to-End Jitter Simulations of the Linac Coherent Light Source", in *Proc. of PAC 2001*, Chicago, IL, USA, 2001, paper WPPH103.

- [3] S. Heifets *et al.*, “Coherent synchrotron radiation instability in a bunch compressor”, *Phys. Rev. ST Accel. Beams*, vol. 5, p. 064401, 2002.
- [4] Z. Huang and K.-J. Kim, “Formulas for coherent synchrotron radiation microbunching in a bunch compressor chicane”, *Phys. Rev. ST Accel. Beams*, vol. 5, p. 074401, 2002.
- [5] S. Abeyratne *et al.*, MEIC Design Summary, <https://arxiv.org/abs/1504.07961>
- [6] C. Tennant and D. Douglas, “Coherent synchrotron radiation induced beam degradation in the MEIC Circulator Cooler Ring”, JLAB-TN-12-027.
- [7] E. Nissen *et al.*, “Microbunching effects induced by CSR in the MEIC Circulator Cooler Ring”, unpublished.
- [8] C.-Y. Tsai, “Growth of density modulation in MEIC CCR due to coherent synchrotron radiation”, presented at EIC’14 (poster).
- [9] C.-Y. Tsai *et al.*, “Linear microbunching gain estimation including CSR and LSC impedances in recirculation machines”, in *Proc. of ERL2015*, Stony Brook, NY, June 2015, paper TUICLH2034.
- [10] D. Douglas *et al.*, “Control of coherent synchrotron radiation and microbunching effects during transport of high brightness electron beams”, [arXiv: 1403.2318v1](https://arxiv.org/abs/1403.2318v1) [physics.acc-ph]
- [11] C.-Y. Tsai *et al.*, “Theoretical Investigation of Coherent Synchrotron Radiation Induced Microbunching Instability for High-Energy Recirculation Arcs”, MEIC Circulator Cooling Ring, and a Novel Compressor Arc: Benchmarking, Stage Gain Analysis, and Parametric Studies, JLAB-TN-16-030.
- [12] C.-Y. Tsai *et al.*, “Theoretical investigation of coherent synchrotron radiation induced microbunching instability in transport and recirculation arcs”, in *Proc. of FEL’14*, Basel, Switzerland, August 2014, paper THP022.
- [13] C.-Y. Tsai *et al.*, “Multistage CSR microbunching gain development in transport and recirculation arcs”, in *Proc. of FEL’15*, Daejeon, Korea, August 2015, paper MOP087.
- [14] C.-Y. Tsai *et al.*, “CSR induced microbunching gain estimation including transient effects in transport and recirculation arcs”, in *Proc. of IPAC’15*, Richmond, VA, USA, May, 2015, paper MOPMA028.
- [15] C.-Y. Tsai *et al.*, “Conditions for CSR microbunching gain suppression”, *Proc. of IPAC’16*, Busan, Korea, May 2016, paper TUOAB02.
- [16] Ya. Derbenev, “Cooling with Magnetized Electron Beam”, presented at the MEIC Spring Collaboration meeting, March 30, 2015. <https://www.jlab.org/conferences/meic15/talks/derbenev.pptx>
- [17] V. Parkhomchuk and I. Ben-Zvi, “Electron Cooling for RHIC”, C-A/AP/47, April 2001, https://www.bnl.gov/cad/ardd/ecooling/docs/PDF/AP_notes/ap_note_47.pdf
- [18] Ya. Derbenev, “A Method to Overcome Space Charge at Injection”, *AIP Conf. Proc.*, vol. 773, p. 335, 2005.
- [19] M. Borland, “elegant: A Flexible SDDS-Compliant Program for Accelerator Simulation,” APS Light Source Note LS-287, September 2000, https://www1.aps.anl.gov/icms_files/lsnotes/files/APS_1418218.pdf
- [20] A. Dragt *et al.*, “Theory of emittance invariants,” *Frontiers of Particle Beams; Observation, Diagnosis and Correction, Lecture Notes in Physics*, vol. 343, pp. 94-121, 1989, doi: 10.1007/Bfb0018283.
- [21] A. Burov *et al.*, “Optical principles of beam transport for relativistic electron cooling”, *Phys. Rev. ST Accel. Beams*, vol. 3, p. 094002, 2000.
- [22] D. Douglas and C. Tennant, “Betatron matching magnetized beams”, JLAB-TN-15-026.
- [23] D. Douglas, “Twiss parameterization of flat beam transforms including beam divergence”, JLAB-TN-15-022.
- [24] M. Borland, “Modeling the microbunching instability”, *Phys. Rev. ST Accel. Beams*, vol. 11, p. 030701, 2008.
- [25] C.-Y. Tsai and R. Li, “Simulation of coherent synchrotron radiation induced microbunching gain using ELEGANT”, JLAB-TN-14-016.
- [26] Ya. S. Derbenev *et al.*, “Microbunch radiative tail-head interaction”, TESLA-FEL-Report 1995-05, https://flash.desy.de/sites2009/site_vuvfel/content/e403/e1642/e1488/e1490/infoboxContent2098/tesla-fel1995-05.pdf
- [27] J. B. Murphy *et al.*, “Longitudinal wakefield for an electron moving on a circular orbit”, *Part. Accel.*, vol. 57, pp. 9-64, 1997.
- [28] R. Li, “Curvature-induced bunch self-interaction for an energy-chirped bunch in magnetic bends”, *Phys. Rev. ST Accel. Beams*, vol. 11, p. 024401, 2008.
- [29] Ya. Derbenev and V. Shiltsev, “Transverse Effects of Microbunch Radiative Interaction”, SLAC-PUB-7181, 1996, <http://slac.stanford.edu/pubs/slacpubs/7000/slac-pub-7181.pdf>
- [30] Landau damping by energy spread is relatively small since $R_{56}\sigma_\delta \approx 80\mu\text{m}$. Compared with the early design of CCR (see Refs. [1, 6, 7]), $R_{51}\sigma_x \approx 10\mu\text{m}$ and $R_{56}\sigma_\delta \approx 30\mu\text{m}$. The maximal gain of CCR occurs at $\lambda \approx 350\mu\text{m}$.